Available online at www.sciencedirect.com
ScienceDirect
Earth and Planetary Science Letters 252 (2006) 379–397
EPSL
www.elsevier.com/locate/epsl

Palaeomagnetic study of Lower Jurassic marine strata from the Neuquén Basin, Argentina: A new Jurassic apparent polar wander path for South America

María Paula Iglesia Llanos [a,*], Alberto Carlos Riccardi [b], Silvia Elisabet Singer [a,1]

[a] *INGEODAV, Depto. Ciencias Geológicas, Fac. Ciencias Exactas y Naturales, Universidad de Buenos Aires, Pab. 2, Ciudad Universitaria, C1428EHA, Buenos Aires, Argentina*

[b] *Invertebrate Palaeontology Department, La Plata Natural Sciences Museum, Paseo del Bosque s/n, 1900, La Plata, Argentina*

Received 14 June 2006; received in revised form 25 September 2006; accepted 1 October 2006
Available online 15 November 2006
Editor: G.D. Price

Abstract

A thorough palaeomagnetic study in four marine sedimentary sections from the Neuquén Basin in west-central Argentina was carried out. Sections are several hundreds meters-thick and consist of ammonite-bearing beds with intercalated volcanics. Two magnetic components carried by titanomagnetites were identified in the studied sections, one soft corresponding most likely to a present-day remagnetisation and a harder one which is interpreted as the primary magnetisation of the sections, based on optical studies and the results of field tests of palaeomagnetic stability, bearing an Early Jurassic age. As a result, two new palaeomagnetic poles for stable South America are presented: one for the Hettangian–Sinemurian located at 223° E, 51° S, A_{95}=6°, N=25, and the other for the Pliensbachian–Toarcian located at 67° E, 74° S, A_{95}=5°, N=52. These and other poles from the literature were used in this study to construct a refined Late Triassic to Jurassic APW path for stable South America, which differs significantly from previous models in showing a cusp between the Sinemurian and the Pliensbachian, indicative of large apparent polar wander. The same feature is observed in other continents of Pangea, like Eurasia. Palaeolatitudes of the Neuquén Basin indicate that South America was subject to considerable N–S movements during the Late Triassic and lowermost Early Jurassic. These latitudinal movements of Pangea are consistent with displacements recorded for marine faunas from South America and Eurasia.

Keywords: Jurassic; palaeomagnetism; Neuquén; Argentina

1. Introduction

Jurassic apparent polar wander (APW) paths from the Atlantic-bordering continents are subject to constant revision due to the fact that many of the constituent palaeomagnetic poles yield controversial rock/magnetisation ages and/or derive from highly deformed areas [e.g. 1–4]. Moreover, possible intracontinental movements [5] may introduce further uncertainties. The great majority of the South American Jurassic palaeopoles were obtained in Patagonia from volcanic [e.g. 6–10] and sedimentary [11,12] rocks, the former providing a well-defined group close to the present geographic pole. Therefore, it has commonly been interpreted that during

* Corresponding author. Tel.: +54 11 4576 3300x292; fax: +54 11 4788 3439.
E-mail addresses: mpiglesia@gl.fcen.uba.ar (M.P.I. Llanos), riccardi@museo.fcnym.unlp.edu.ar (A.C. Riccardi), singer@gl.fcen.uba.ar (S.E. Singer).
[1] Fax: +54 11 4788 3439.

0012-821X/$ - see front matter © 2006 Elsevier B.V. All rights reserved.
doi:10.1016/j.epsl.2006.10.006

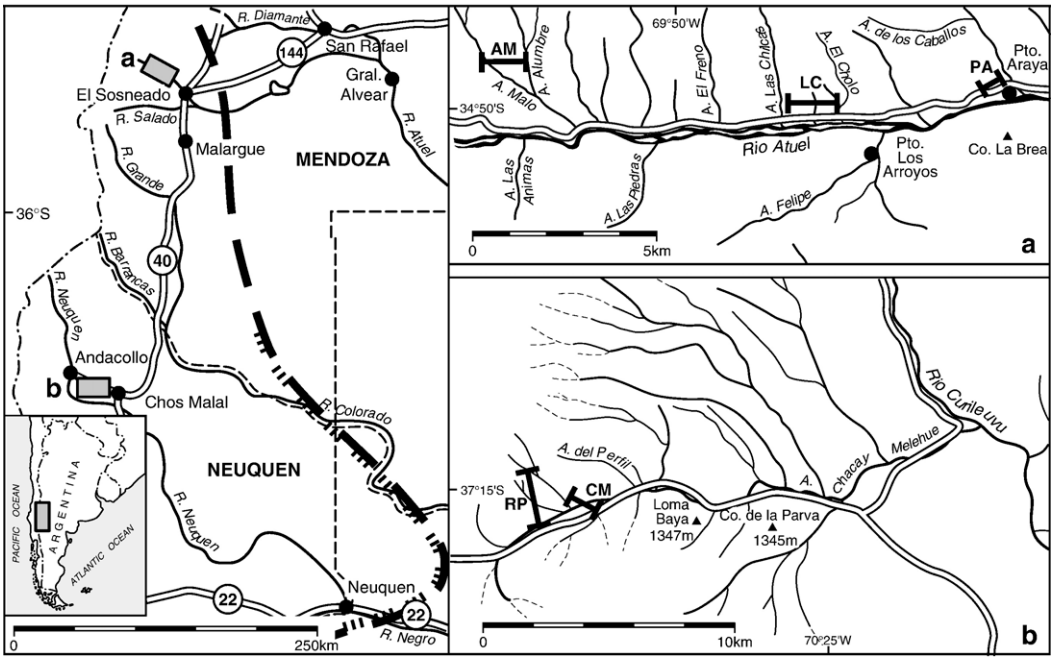

Fig. 1. Sketch map of the Neuquén Basin and detail of the studied localities. a: Arroyo Malo (AM), Las Chilcas (LC) and Puesto Araya (PA), b: Rajapalo–Chacay Melehue (RP–CM). Thick dashed line: eastern border of the Basin.

the Middle to Late Mesozoic, APW of stable South America was small [13–16]. This conclusion however, has been questioned by some authors [e.g. 11,12,17] on the basis of new and reassessed literature data that reflected significant latitudinal movements and high drift rates for South America during the Early Jurassic.

For this study, we sampled four sections in northern and central Neuquén Basin from west-central Argentina. They are several hundreds meters thick and consist mainly of marine sedimentary beds bearing Early Jurassic ammonites. Field tests of palaeomagnetic stability and magnetic mineral analyses were used to confirm that recorded magnetisations are primary. The resultant palaeomagnetic poles, together with other palaeopoles from the literature, were used to construct a new Jurassic APW path for stable South America.

2. Geological setting and sampling methodology

The sections sampled are located within the Neuquén Basin in west-central Argentina (Fig. 1). This back-arc basin originated in the Triassic due to the break-up of Gondwana [18]. It extends over more than 160,000 km^2 and comprises a *c.* 7 km-thick succession that spans the Mesozoic–Cenozoic, made up of mostly sedimentary rocks with subordinate volcanics. From the Middle Triassic to the Sinemurian a series of unconnected half-grabens developed through basement faults [e.g. 19,20] controlled the subsidence and deposition of the sediments. Sedimentation began in the Triassic with volcanic and continental coarse-grained deposits and during the Late Triassic, the first trangression from the Pacific Ocean occurred across the volcanic arc, as a narrow corridor which is exposed in the locality of Arroyo Malo-Arroyo Alumbre in the northern part of the basin (Fig. 1a). Subsequently, the onset of the sag phase [20] determined the coalescence of these grabens and the consequent flooding of the basin in the Pliensbachian [21]. During the Pliensbachian–Toarcian, a westward prograding clastic system developed which comprised nearshore sandstones and offshore shales, sporadically interrupted by volcanic deposits.

Jurassic sections in the Neuquén Basin bear ammonites which are correlatable with the European Standard Zonation (Fig. 2). Hence, on this basis we can tie our polarity zones to those of the International Geomagnetic Polarity Time Scale [22], thus obtaining a precise temporal record of the sampled successions.

The four sampled marine sections spanning the Hettangian–Toarcian are located in the north (Arroyo Malo, Las Chilcas and Puesto Araya) and centre (Rajapalo–Chacay Melehue) of the basin (Fig. 1). The whole Early Jurassic succession has been folded during the Andean Orogeny (Cretaceous–Tertiary) producing

STANDARD ZONATION			NEUQUEN BASIN	
STAGES		ZONES	ASSEMBLAGE ZONES	
TOARCIAN	U	LEVESQUEI	Dumortieria	Z20
			Phlyseogrammoceras tenuicostatum	Z19
		THOUARSENSE	Phymatoceras	Z18
		VARIABILIS	Collina chilensis	Z17
	L		Peronoceras pacificum	Z16
		BIFRONS	Peronoceras largaense	Z15
		FALCIFERUM	Dactylioceras hoelderi	Z14
		TENUICOSTATUM	Tenuicostatum	Z13
PLIENSBACHIAN	U	SPINATUM	Fanninoceras disciforme	Z12
		MARGARITATUS	Fanninoceras fannini	Z11
	L	DAVOEI	Fanninoceras behrendseni	Z10
			Dubariceras	Z9
		IBEX	Tropidoceras	Z8
		JAMESONI	Miltoceras	Z7
SINEMURIAN	U	RARICOSTATUM	"Epophioceras"	Z6
		OXYNOTUM		
		OBTUSUM		
	L	TURNERI	?	
		SEMICOSTATUM	"Agassiceras"	Z5
		BUCKLANDI		
HETTANGIAN		ANGULATA	"Vermiceras"	Z4
			Badouxia canadensis	Z3
		LIASICUS	"Waehneroceras-Schlotheimia"	Z2
			Kammerkarites bayoensis	Z1
		PLANORBIS	Psiloceras rectocostatum	
			?	
TRIASSIC U	RHAETIAN	MARSHI	Choristoceras	
		SUESSI		

Fig. 2. Proposed correlation between the Standard and the Andean ammonite Zones in the Upper Triassic–Lower Jurassic.

N–S oriented structures. Bedding attitudes are displayed in Tables 1 (Hettangian–Sinemurian) and 2 (Pliensbachian–Toarcian). For the palaeomagnetic sampling, we favoured fine-grained sediments and volcanics. At least two hand samples were collected from which four specimens were obtained at each sampling level. The average distance between levels was 10 m, well within ammonite biozone ranges.

To the north of the basin along the Atuel River (Fig. 1a), is exposed a *c*. 2 km-thick Late Triassic to Toarcian marine succession. It is composed of transgressive deposits which become younger and coarser-grained to the east. Thus to the west of Arroyo El Freno (Fig. 1a), the sedimentary section cropping out at Arroyo Malo (AM) records syn-rift phases and forestepping fault-controlled, fluvio-dominated slope-type fan deltas whereas to the east of the El Freno at Las Chilcas (LC) and Puesto Araya (PA) sections register transgressive storm-dominated shelf deposits, indicative of sag phases [23]. In Arroyo Malo (34°48′ S, 69°54′ W) the Upper Triassic–Lower Sinemurian succession (Fig. 3) is *c.*1 km-thick and includes from base to top, the Arroyo Malo, El Freno and El Cholo Formations [24–27]. The shales and sandstones of the Arroyo Malo Formation bear ammonites recording (Fig. 2) the Choristoceras to Rectocostatum Zones that can be correlated with the European Marshi (Late Rhaetian) to Planorbis (Early Hettangian) Zones. Above follow fluvial conglomerates and sandstones of the El Freno Fm. On top, the shales and sandstones of the El Cholo Fm. bear ammonites (Fig. 2) of the Kammerkarites bayoensis to "Agassiceras" Zones which are correlatable with the uppermost Planorbis-lower Liasicus (Early–Middle Hettangian) to Semicostatum (Early Sinemurian) Zones. Intercalated in the El Cholo Fm., there are at least three alkaline sills, the lowermost basaltic and the others lamprophyric.

The 500 m-thick section at Las Chilcas (34°54′ S, 69°48′ W) is divided (Fig. 3) in the El Freno and El Cholo Formations. The first is thicker, coarser-grained and younger than in Arroyo Malo, probably Sinemurian. The El Cholo Fm. comprises shales and sandstones with ammonites of the "Epophioceras" and Miltoceras Zones that are equivalent (Fig. 2) to the Turneri (Early Sinemurian) to Jamesoni (Early Pliensbachian) Standard Zones. A lamprophyric sill is intercalated in the El Cholo Fm. at *c.* 300 m from the base (Fig. 3), marking the cessation of alkaline intrusions in the area. Hence these sills, that were intruded during the first stages of the rifting, bear an Hettangian–Sinemurian age.

The occurrence in these sections of flattened shale concretions, ammonites and sedimentary structures such as convolute bedding, water escape, load textures within the Hettangian–Sinemurian interval of El Cholo Fm., are indicative of significant compaction due to sedimentary overload. Moreover, deformed ammonites therein show compaction values of up to 66% with respect to undeformed specimens of the same species. Pliensbachian–

Table 1
Geological and palaeomagnetic data of sampling sites at the Hettangian–Sinemurian localities Arroyo Malo and Las Chilcas

Locality Lat., Long.	Site (m from the base)	Lithology	Formation	Biozone	n/N		ChRM Dc, Io	I_s	α_{95}	k	VGP Lat S, Long E	Tilt cor. Strike, dip
						$J_r(A/m)$						
Las Chilcas	348	Sediments	El Cholo	Epophioceras	5/1	$4.2\ 10^{-4}$	249.6, 71.2	56.8	–	–	39.3, 247.2	173, 29
34°54′S, 69°48′W	320	Sediments	″	″	6/2	$2.6\ 10^{-4}$	251.1, 49.5	31.3	–	–	31.2, 217.5	″
	307.3	Volcanics	″	″	3/2	$5.0\ 10^{-3}$	231.5, 46.9	–	–	–	46.0, 206.2	″
	307.1	Volcanics	″	″	4/4	$8.6\ 10^{-4}$	244.0, 56.7	–	11.3°	66.9	39.2, 222.8	″
	307	Volcanics	″	″	3/3	$4.9\ 10^{-3}$	211.9, 63.7	–	1.6°	5722.1	63.7, 233.3	″
	−1	Sediments	El Freno	″	4/1	$5.4\ 10^{-4}$	48.3, −69.4	−54.2	–	–	51.7, 243.8	184, 39.6
Arroyo Malo	1019	Sediments	El Cholo	Agassiceras?	6/1	$2.9\ 10^{-4}$	54.2, −71.7	−57.5	–	–	47.8, 248.3	184, 43
34°48′S, 69°54′W	834	Sediments	″	Agassiceras	6/2	$2.3\ 10^{-4}$	30.1, −53.8	−35.4	–	–	65.3, 207.7	″
	826	Sediments	″	″	6/1	$4.7\ 10^{-4}$	45.6, −69.2	−53.8	–	–	53.3, 243.7	″
	783	Sediments	″	″	4/2	$7.4\ 10^{-4}$	57.1, −51.2	−32.9	–	–	42.9, 213.5	″
	766	Sediments	″	″	2/2	$5.0\ 10^{-4}$	45.9, −57.6	−39.3	–	–	53.3, 219.3	″
	750	Sediments	″	″	1/1	$6.9\ 10^{-4}$	25.4, −44.3	−26.9	–	–	66.5, 185.1	″
	695	Sediments	″	″	2/2	$3.9\ 10^{-4}$	48.7, −50.3	−32.1	–	–	49.4, 209.0	″
	690	Sediments	″	″	4/3	$4.0\ 10^{-4}$	29.7, −64.4	−47.4	–	–	64.9, 236.2	″
	610	Volcanics	″	Vermiceras	2/1	$1.5\ 10^{-3}$	214.8, 57	–	–	–	61.9, 216.1	″
	580	Volcanics	″	″	3/1	$1.2\ 10^{-2}$	224.4, 75.3	–	–	–	51.1, 258.9	″
	578	Volcanics	″	″	4/4	$1.4\ 10^{-2}$	223.2, 63.9	–	6.7°	187.2	55.7, 231.8	181, 57.5
	492	Sediments	″	Badouxia canadensis	4/1	$2.4\ 10^{-4}$	54.5, −53.9	−35.5	–	–	45.7, 216.0	″
	429	Sediments	″	Waehneroceras–Schlotheimia	6/2	$8.0\ 10^{-3}$	238.1, 41.6	24.8	–	–	38.9, 204.3	″
	427	Volcanics	″	″	5/5	$1.6\ 10^{-2}$	48.3, −45.7	–	12.8°	36.5	48.3, 203.2	″
	357	Sediments	″	″	3/1	$2.2\ 10^{-4}$	228.1, 41.6	24.8	–	–	47.1, 198.8	″
	300	Sediments	″	Psiloceras	5/2	$2.4\ 10^{-4}$	234.5, 49	30.9	–	–	44.3, 209.9	″
	246.5	Sediments	Arroyo Malo	″	1/1	$1.8\ 10^{-4}$	64.7, −51.5	−33.2	–	–	36.9, 216.9	155, 52
	201.5	Sediments	″	″	1/1	$2.6\ 10^{-4}$	210.1, 64.6	47.6	–	–	64.5, 236.6	″
	199.5	Sediments	″	″	1/1	$2.5\ 10^{-4}$	266.9, 63.9	46.7	–	–	26.0, 239.1	″

Symbols: n/N=total /selected samples; Jr=natural remanent magnetisation intensity; ChRM=characteristic remanent magnetisation; D_c, I_o=declination, inclination after bedding and inclination error-correction; I_s=inclination without the inclination error-correction, α_{95}=semi-angle of confidence; k=Fisher's precision parameter; VGP=virtual geomagnetic pole; Bedding correction = Strike follows the right-hand rule.

Toarcian successions were sampled at Puesto Araya (PA, Fig. 1a) and Rajapalo–Chacay Melehue (RP–CM, Fig. 1b). In Puesto Araya (34°57′S, 69°42′W), the *c.* 400 m-thick succession is composed (Fig. 4) of well-bedded, fining-and thinning-upward sandstones and shales representative of transgressive storm-dominated shelf facies [23]. It comprises from base to top, the El Freno and El Cholo Formations. El Freno consists of coarse-grained sandstones and conglomerates and is probably slightly younger than in Las Chilcas [28]. The overlying El Cholo [29–32] is made up of sandstones and shales with ammonites that record (Fig. 2) the Tropidoceras to Fanninoceras fannini Zones correlatable with the European uppermost Jamesoni (Early Pliensbachian) to Margaritatus (Late Pliensbachian) Zones. Further to the south of the basin, the Rajapalo–Chacay Melehue section (Fig. 1b) begins [33–35] with (Fig. 4) a pre-Jurassic? volcanic basement, on top of which lies a *c.* 500 m-thick succession of marginal marine to off-shore deposits corresponding to the Lista Blanca and Los Molles Formations. The Lista Blanca Fm. is made up of tuffs, flows and sandstones and bears ammonites (Fig. 2) of the Fanninoceras disciforme Zone, which is partially equivalent to the Margaritatus–Spinatum (Late Pliensbachian) Standard Zones. The Los Molles Fm. consists of shales with minor tuffs and ignimbrites bearing ammonites of the Dactylioceras hoelderi and Peronoceras largaense Zones that are partially equivalent to the Falciferum to Early Bifrons (Early Toarcian) Standard Zones.

3. Petrography

Optical observations under transmitted and reflected light were performed in representative lithologies, in order to study the minerals and in particular to identify the magnetic ones.

3.1. Hettangian–Sinemurian

In Arroyo Malo (Fig. 3), polished sections from siltstones show titanomagnetite as a common opaque mineral, partially oxidised to titanohaematite. Despite the oxidation observed in the samples, ilmenomagnetite crystals (9 to 25 μ) are of volcanic origin and were formed at temperatures above 600 °C, as shown by the distinct textures and plastic deformation of the grains. Mineral assemblages of rocks include albite, titanite, carbonate, epidote and chlorite, indicative of greenschist facies caused by hydrothermal metamorphism. On the other hand, the lower sill (AM10, Fig. 3) is an alkaline metabasalt (Fig. 5a) with porphyritic texture. Phenocrysts are pseudomorphs of olivine that include carbonates and opaque minerals, and the groundmass consist of plagioclase, clinopyroxene, alkaline amphibole, opaque minerals, carbonate, chlorite and titanite. Under reflected light, abundant large ilmenite (<120 μ) with subordinate pyrite and small magnetite crystals (<10 μ) are observed. The latter are contained within the olivines as optically homogeneous equant grains that formed due to the hydrothermal alteration of silicates, soon after the rock formation. These magnetite crystals, in our view, represent a pure-type and behaved as an optimal recorder of the Jurassic palaeomagnetic field. Another sill in the same section (AM21, Fig. 3) is a lamprophyre which, under transmitted light, shows (Fig. 5b) a porphyritic texture. Phenocrysts consist of two populations, one Ti-rich alkaline amphibole (Ti-rich kaersutite?) and the other, clinopyroxene, and the groundmass includes plagioclase with often destroyed primary twins (albite?), clinopyroxene, apatite, titanite, carbonate, chlorite, epidote and few opaque minerals (titanomagnetite?). Under reflected light, the dominant oxide is ilmenite with subordinate amounts of relict titanomagnetite as well as pyrite altered to limonites. A similar lamprophyric rock is found in a sill intercalated in the Las Chilcas section (LC5, Fig. 3).

3.2. Pliensbachian–Toarcian

Representative lithologies of this age were studied in the Rajapalo section (Fig. 4). Sedimentary rocks correspond to medium-grained sandstones whose angular clasts consist of lava and glass embedded in a fine groundmass of quartz, chlorite, calcite that includes altered angular fragments (shells?). Under reflected light, idiomorphic rutile, magnetite crystals (20 to 50 μ) and secondary titanium minerals are observed. The latter are the most common minerals in the pyroclastic rocks of this section. On the other hand, basalts (RP36, Fig. 4) contain (Fig. 5c) large amounts of titanomagnetite with equant and octahedral habits (from 25 μ to below the microscope resolution limit), in which rapid quenching prevented high temperature oxidation and resulted in the fine grain size that makes these basalts excellent palaeomagnetic recorders.

4. Palaeomagnetic results

Palaeomagnetic studies were performed at INGEODAV, Universidad de Buenos Aires, using a TSD-1 Schonstedt oven and a static 2G alternating field (AF) device for demagnetisation of specimens, as well as a 2G (DC squids) cryogenic magnetometer for measurement of the magnetic

Table 2
Geological and palaeomagnetic data of sampling sites at the Pliensbachian–Toarcian localities Puesto Araya and Rajapalo–Chacay Melehue

Locality Lat., Long.	Site (m from the base)	Lithology	Formation	Biozone	n/N	ChRM $J_r(A/m)$	ChRM D_t, I_t	α_{95}	k	VGP Lat S, Long E	Tilt cor. Strike, dip
Chacay Melehue	68	Sediments	Los Molles	Peronoceras Iargaense	4/1	$2.9\ 10^{-4}$	329.9, −38.4	–	–	59.7, 42.1	61.27
37°16′ S, 70°27′ W	45	″	″	Dactylioceras hoelderi	6/1	$7.1\ 10^{-5}$	18.6, −48.2	–	–	72.5, 177.5	″
	28	″	″	″	4/4	$5.1\ 10^{-4}$	343.8, −35.4	8.2°	126.5	67.3, 66.5	″
	26	″	″	″	3/2	$8.4\ 10^{-5}$	354.0, −34.3	–	–	70.8, 92.0	″
	22	″	″	″	2/2	$1.3\ 10^{-4}$	338.3, −35.7	–	–	64.2, 56.4	″
	18	″	Lista Blanca	″	6/2	$3.8\ 10^{-5}$	20.1, −40.8	–	–	67.8, 166.3	″
	12	″	″	″	6/2	$1.1\ 10^{-4}$	6.2, −59.9	–	–	84, 237.5	″
	10	″	″	″	4/2	$1.3\ 10^{-5}$	46.2, −33.6	–	–	45.5, 187.4	″
Rajapalo	313	Sediments	Los Molles	Dactylioceras hoelderi	5/1	$1.1\ 10^{-3}$	351.1, −52.0	–	–	81.4, 49.5	61, 27
37°16′ S, 70°27′ W	297	″	″	″	4/1	$2.6\ 10^{-4}$	140.1, 71.1	–	–	57.6, 332.1	″
	293	″	″	″	5/2	$1.0\ 10^{-3}$	166.2, 51.4	–	–	77.5, 40.1	″
	290	″	″	″	3/1	$5.3\ 10^{-4}$	164.6, 51.4	–	–	76.3, 37.4	″
	270	″	″	″	6/5	$2.1\ 10^{-4}$	355.0, −32.9	8.1°	89.6	70.2, 95.4	″
	263	″	″	″	5/5	$1.1\ 10^{-3}$	348.7, −25.3	10.5°	54.4	64.0, 83.8	″
	257	Volcaniclastics	Lista Blanca	?	4/4	$1.6\ 10^{-3}$	352.5, −19.6	8.8°	109.3	62.0, 93.7	″
	233	″	″	?	4/1	$2.7\ 10^{-4}$	347.9, −48.9	–	–	77.5, 52.5	″
	183	″	″	?	6/4	$7.4\ 10^{-5}$	171.6, 52.1	9.1°	102.0	81.8, 50.6	″
	180	″	″	?	7/6	$1.4\ 10^{-3}$	344.1, −43.8	13.1°	27.0	72.2, 55.8	″
	170	Sediments	″	?	7/6	$2.9\ 10^{-4}$	341.3, −44.9	7.6°	79.0	70.9, 48.5	″
	138	Volcaniclastics	″	?	5/2	$3.3\ 10^{-4}$	336.0, −40.2	–	–	64.9, 47.6	″
	117	″	″	?	3/2	$3.7\ 10^{-4}$	343.0, −27.1	–	–	62.5, 71.6	″
	110	″	″	?	4/3	$2.3\ 10^{-3}$	351.9, −42.1	7.7°	260.1	75.3, 79.1	″
	103	″	″	?	8/8	$2.5\ 10^{-3}$	345.1, −48.1	5.2°	114.5	75.1, 48.4	″
	97	″	″	?	5/3	$3.3\ 10^{-3}$	342.6, −50.9	5.3°	544.7	74.6, 36.0	″

	78	Volcanics	″	–	6/6	$1.8\ 10^{-3}$	337.3, −46.0	14.3°	23.0	68.5, 40.4	″
	77	″	″	–	7/4	$1.2\ 10^{-3}$	187.2, 40.4	14.7°	40.0	74.5, 135.1	″
	75	″	″	–	7/5	$1.4\ 10^{-1}$	188.2, 42.8	13.9°	31.3	75.7, 141.3	″
	70	″	″	–	3/3	12.0	176.4, 35.1	10.4°	140.5	71.8, 98.6	″
	66	″	″	–	11/11	$2.7\ 10^{-1}$	189.2, 41.0	6.8°	45.8	74.1, 142.0	″
	62	″	″	–	2/1	$9.6\ 10^{-2}$	213.2, 21.0	–	–	50.2, 166.7	″
	60	″	″	–	6/6	3.8	186.3, 27.5	7.3°	84.6	66.6, 125.1	″
	57	Volcaniclastics	″	Fanninoceras disciforme	8/5	$9.2\ 10^{-3}$	340.7, −44.1	10.6°	53.0	70.0, 48.9	″
	34	″	″	″	10/9	$3.9\ 10^{-3}$	344.4, −53.2	11.8°	20.0	76.8, 30.4	″
	5	Volcanics	″	″	7/5	$4.3\ 10^{-2}$	172.2, 43.8	7.6°	101.8	76.6, 77.7	″
	0	″	No name	–	2/1	$3.0\ 10^{-2}$	344.1, −20.3	–	–	59.6, 77.4	″
	−6	″	″	–	8/5	$1.4\ 10^{-1}$	352.5, −27.5	12.3°	39.5	66.4, 91.2	″
	−10	″	″	–	6/4	$8.2\ 10^{-2}$	168.3, 41.6	8.0°	132.0	73.3, 69.3	″
Puesto Araya	333	Sediments	El Cholo	?	6/6	$8.9\ 10^{-4}$	347.8, −40.1	9.9°	47.1	73.9, 65.8	1, 42.5
34°57′ S, 69°42′ W	320	″	″	?	6/4	$1.3\ 10^{-3}$	332.5, −40.4	12.5°	55.1	63.3, 39.3	″
	279	″	″	?	6/2	$1.6\ 10^{-3}$	202.4, 31.7	–	–	63.3, 164.3	″
	199	″	″	Fanninoceras fannini	4/3	$1.1\ 10^{-3}$	331.3, −31.7	10.4°	141.6	58.9, 47.7	357, 31.5
	187	″	″	F. Behrendseni	4/4	$6.5\ 10^{-4}$	349.2, −44.6	9.2°	99.7	77.3, 60.5	″
	176	″	″	″	6/5	$1.0\ 10^{-3}$	341.7, −41.2	14.0°	31.0	70.5, 50.8	″
	138	″	″	Dubariceras	2/2	$8.2\ 10^{-4}$	323.2, −35.8	–	–	54.3, 35.5	349, 30
	54	″	″	Tropidoceras	2/2	$1.1\ 10^{-3}$	318.1, −52.3	–	–	55.4, 11.5	″
	45.2	″	″	?	3/2	$7.1\ 10^{-4}$	156.6, 7.2	–	–	51.9, 70.3	342, 37
	45	″	″	?	1/1	$3.0\ 10^{-4}$	304.5, −40.9	–	–	40.8, 18.2	″
	40.2	″	″	?	1/1	$6.9\ 10^{-4}$	165.0, 24.0	–	–	63.8, 75.4	″
	40	″	″	?	3/3	$1.1\ 10^{-2}$	299.2, −44.0	9.4°	172.2	37.5, 12.7	″
	20	″	″	?	4/3	$1.4\ 10^{-3}$	357.8, −36.7	10.0°	154.5	75.4, 102.1	″
	15	″	″	?	4/2	$8.0\ 10^{-4}$	150.0, 19.0	–	–	52.8, 55.7	″

D_t, I_t = declination, inclination after bedding-correction. Other symbols as in Table 1.

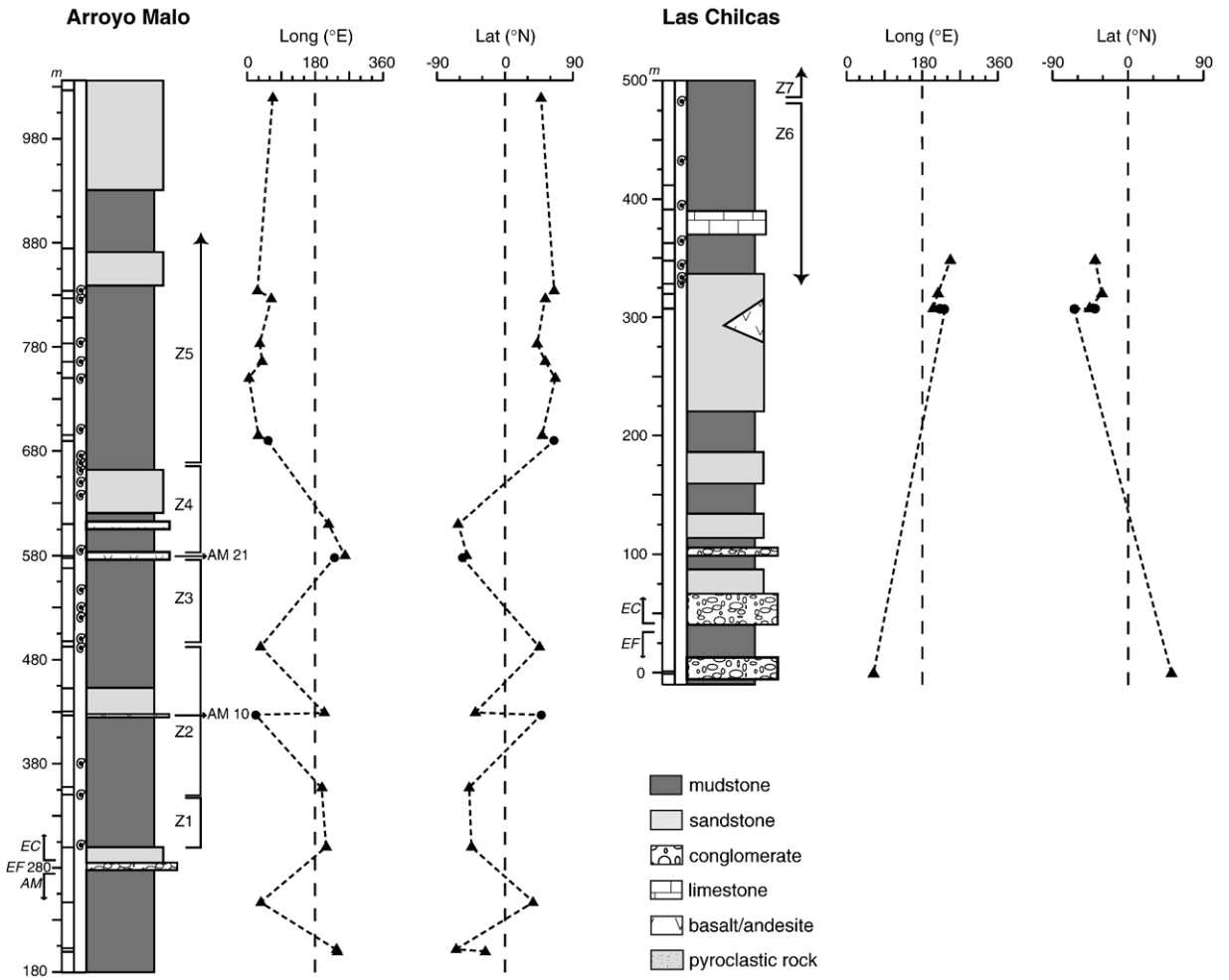

Fig. 3. Stratigraphical columns, sampling sites and virtual geomagnetic poles (VGP) of the studied Hettangian–Sinemurian sections at Arroyo Malo and Las Chilcas. Data show position of (left) ammonites and palaeomagnetic sampling sites and (right) Ammonite Assemblage Zones (in Fig. 2), petrographical samples and VGP (in Table 1). Symbols = circles (triangles) sampling sites with $N \geq 3$ ($N \leq 2$), *AM*: Arroyo Malo Fm., *EF*: El Freno Fm., *EC*: El Cholo Fm.

remanence. The software used for the data analysis was developed in Buenos Aires and Utrecht Universities.

Specimens were subject to ten demagnetisation steps on average, with maximum temperatures of 550–580 °C, occasionally 700 °C, and maximum fields of 130 mT. After each thermal demagnetisation step, we measured bulk magnetic susceptibility (X) of specimens to detect the formation of new magnetic minerals. In general, X is on the order of 1×10^{-4} SI for sediments and 6×10^{-4} SI for volcanics, except for basalts in Rajapalo (Fig. 4) where this parameter is considerably higher (up to 1×10 SI). Above 500–550 °C, X increased significantly in most samples and magnetic behaviours became erratic. Thus we preferred the AF method even though in many samples the maximum available field (130 mT) could not remove the residual magnetisation completely, due to occurrence of secondary high coercive mineral(s) (titanohaematite?).

Palaeomagnetic behaviours were quite variable, even within-site. Thus, we observed specimens showing characteristic components with trajectories to the origin, others with curved trajectories defining great circles, and finally other specimens with fully unstable behaviours. The latter represented approximately 50% of the total samples in the case of the Hettangian–Sinemurian (see Table 1) and 30% in the case of the Pliensbachian–Toarcian (Table 2), and were not considered in this study. Therefore, we will refer herein only to specimens that were analysed using principal component analysis [36].

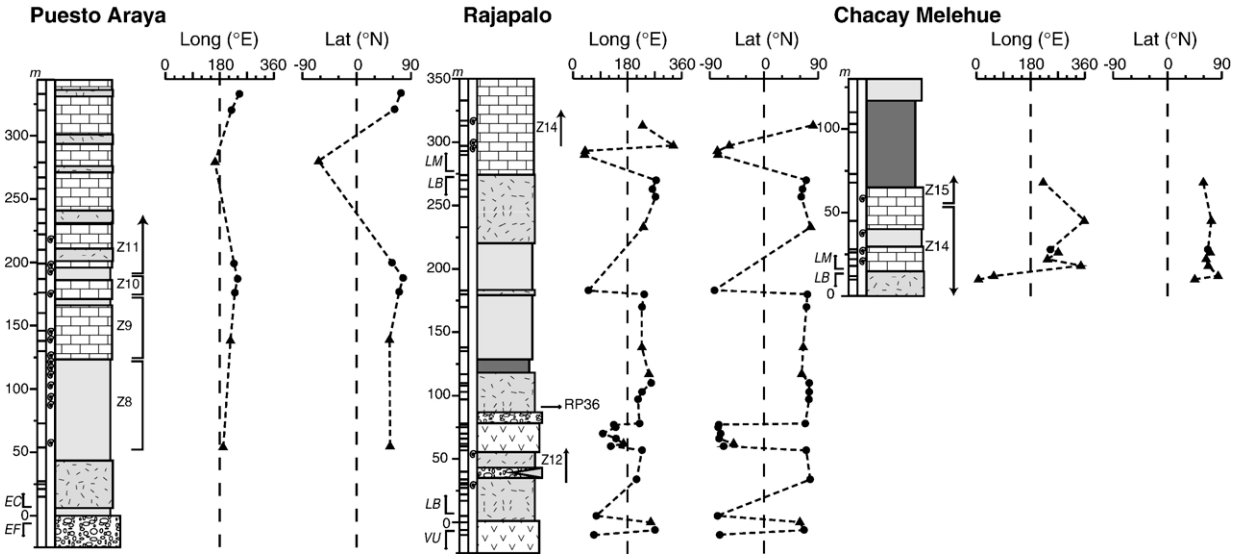

Fig. 4. Stratigraphical columns, sampling sites and VGP of the studied Pliensbachian–Toarcian sections at Puesto Araya and Rajapalo–Chacay Melehue. *VU*: volcanic unit (unnamed), *LB*: Lista Blanca Fm., *LM*: Los Molles Fm. Symbols as in Fig. 3.

The great majority of specimens show two magnetic components (Fig. 6). The soft component, labelled "A", is removed by 200–400 °C and up to 20 mT and bears northern declinations with negative inclinations. It is carried by relatively big crystals of titanomagnetite and yields a mean direction that coincides with the present-day local magnetic field (Fig. 7a). Component B on the other hand, is commonly erased (Fig. 6) at 550–580 °C (50 to 60 mT) and, occasionally, 700 °C (more than 130 mT), showing N–NE (S–SW) declinations with negative (positive) inclinations when bedding-corrected (Fig. 7c). This component is carried very likely, by single to pseudo-single domain (poor Ti)-magnetite crystals formed rapidly after the hydrothermal alteration of the rocks in the case of the Hettangian–Sinemurian volcanics (Fig. 5a) or during the lava crystallisation in the case of the Pliensbachian–Toarcian basalts (Fig. 5c) whereas in the case of sedimentary rocks, component B is carried by ilmenomagnetite. To a less extent, this component is carried by a mineral with high coercive forces as well, probably titanohaematite (Fig. 6c).

Site mean directions were calculated using Fisher's [37] statistics. Nearly half of these site means (Tables 1 and 2, Figs. 3 and 4) were derived from three or more specimens (circles) and the other half were calculated from one to two specimens (triangles). Field tests of palaeomagnetic stability were applied in both the Hettangian–Sinemurian and Pliensbachian–Toarcian sections, to examine the origin of the isolated magnetisations (see below).

From mean site directions, virtual geomagnetic poles (VGP) and corresponding palaeomagnetic poles were calculated.

4.1. Hettangian–Sinemurian

In Arroyo Malo and Las Chilcas, component A yields a mean *in situ* direction at: Dec=355.5, Inc=−56, α_{95}=8°, N=45 (Fig. 7a). Component B on the other hand shows a mean *in situ* direction (Fig. 7b) at (Dec=166, Incl=64, α_{95}=7°, k=21, N=25) which moves to NE (SW) declinations when bedding-corrected (Figs. 6 and 7c). In this case, directions clearly fall into two groups separated *c.* 18° in inclination (Fig. 7d), one bearing "low" (mean direction at Dec=231.0, Incl=40.5) values recorded in sedimentary rocks and another with "high" values (mean direction at Dec=226.3, Incl=58.8) derived from the sills. We interpret it as the result of the significant burial compaction underwent by these sections, as observed in ammonites and sedimentary structures, which caused magnetic inclinations in sedimentary rocks to become shallower than the original Jurassic ones preserved in the sills. Hence, directions derived from sedimentary sites clearly required an additional correction. A few corrections have been proposed in the literature for inclination shallowing induced by burial compaction [e.g. 38–40], that involve anisotropy of magnetic susceptibility and anisotropy of remanence measurements which were not possible to apply to our data. Instead, we used King's [41] formula, which relates the "compacted" and the original magnetic

inclinations, derived from sedimentary (I_s, Table 1) and volcanic (I_o, Table 1) sites, respectively, as follows:

$$I_o = \tan^{-1}(\tan I_s / f) \quad (1)$$

An average f value was calculated for the Hettangian–Sinemurian interval of the El Cholo Fm. using the mean directions from sedimentary and volcanic sites, and then applied it to each sedimentary site in order to get the corresponding I_o (Table 1).

In addition, we checked this compaction correction at a Formation level, by introducing the sedimentary and volcanic mean directions from (1), in a polynomial function that represents and empirical relationship between volume loss and inclination shallowing derived from experimental compaction of fine-grained marine sediments (Kodama and Anastasio, pers. comm.). Results show that the volume loss in the Hettangian–Sinemurian interval of the El Cholo Fm. has been between 65 and 70%, thus coinciding with values derived from ammonites. This good agreement supports the validity of the inclination shallowing correction we applied to sedimentary sites.

The mean direction for component B, in the reverse polarity, is Dec=230, Incl=58, α_{95}=4.5°, k=41, N=25 (Fig. 7e), dissimilar to any other younger direction in the locality.

4.1.1. Field tests of palaeomagnetic stability

Component B passes (Fig. 7b,e) McFadden's [42] fold test (minimum test value at 100% of unfolding) indicating that in Arroyo Malo and Las Chilcas it was acquired prior to tectonic deformation. In addition in Arroyo Malo, the component passes the reversal test [43] as class C, indicating that normal and reverse polarity populations are antiparallel. In Las Chilcas on the other hand, the reversal test becomes "indeterminate", due most likely to the scarce data in the reverse polarity population. Finally, component B passes a "baked contact test" (Fig. 8) at site 430 m (*AM 10*, Fig. 3). There, host sedimentary rocks (*AM 7*) carry two components, a soft one with normal polarity acquired most likely during the intrusion of the sill (*AM 9*) and a hard one, bearing the opposite polarity and a direction that is consistent with that of the section (component B).

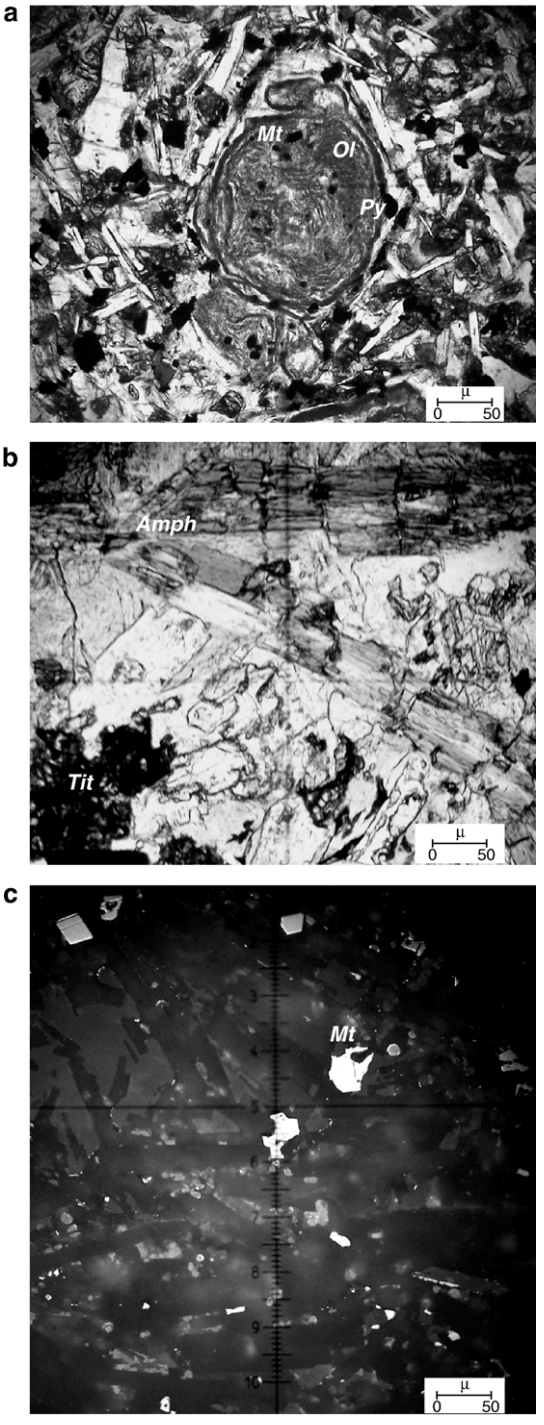

Fig. 5. a) Microphotograph under transmitted light of the lower sill at Arroyo Malo (AM 10, in Fig. 3) showing an alkaline metabasalt, with large amounts of ilmenite and small magnetite (Mt) crystals included in olivine (Ol) phenocrysts as well as pyrite (Py) originated due to the hydrothermal alteration soon after the rock formation. b) Microphotograph under transmitted light of a lamprophyric sill at Arroyo Malo (AM 21, Fig. 3) containing phenocrysts that are made up to a great extent, by alkaline amphibole (Amph) probably kaersutite and titanite (Tit), in a groundmass of chlorite, carbonate, epidote, albite and opaque minerals. c) Microphotograph under reflected light in oil of a basalt at Rajapalo (RP 36, Fig. 4) containing large amounts of magmatic titanomagnetite. This mineral appears as single and pseudo single domain size crystals with equant and octahedral habitus which make them optimal palaeomagnetic recorders.

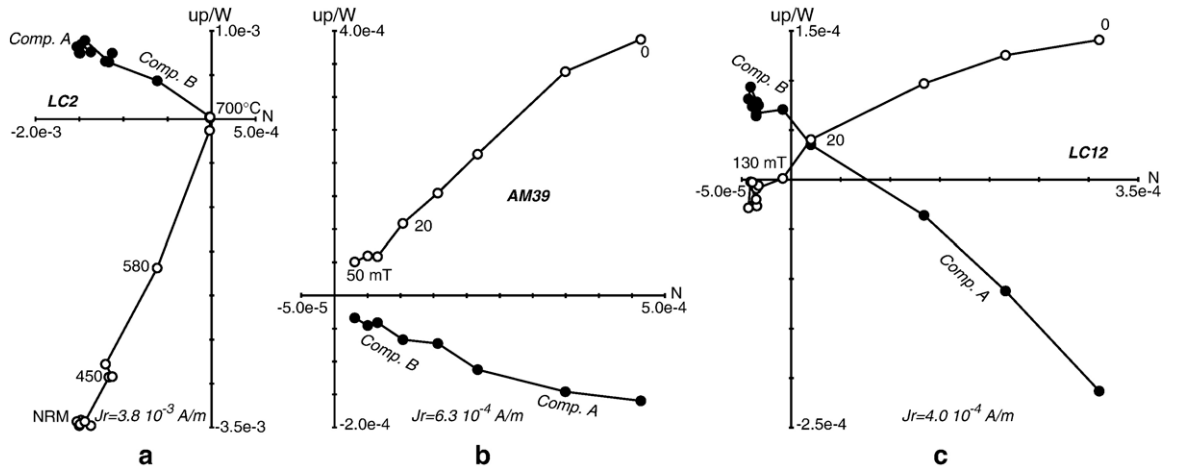

Fig. 6. Representative Zijderveld plots (bedding-corrected) from Hettangian–Sinemurian sedimentary (AM, LC) showing two magnetic components. Component A has N declinations with negative inclinations carried by "soft" titanomagnetites (~400 °C/20 mT), whereas component B shows consistent NE (SW) declinations with negative (positive) inclinations carried by harder titanomagnetites (580 °C/50 mT) and another mineral with higher unblocking temperatures/coercive forces, (~700 °C/ 130 mT), probably titanohaematite. Symbols: full dot = declination; open dot = apparent inclination. *Jr* = NRM intensity in Amperes/meter.

Hence, field tests and petrographical characteristics of the magnetic carriers of component B are solid evidence to interpret that this component is the characteristic Hettangian–Sinemurian magnetisation, acquired during or shortly after the deposition (intrusion) of the sediments (sills) in Arroyo Malo and Las Chilcas.

For component A, VGP derived from specimen directions (*in situ*) yield a PP at 317° E, 85° S, $A_{95}=10°$, $N=45$ that most likely represents the present-day field. For component B, VGP were calculated from site mean directions (Table 1) with the PP located at 223° E, 51° S, $A_{95}=6°$, $N=25$ for the Hettangian–Sinemurian (Table 3).

4.2. Pliensbachian–Toarcian

In Puesto Araya and Rajapalo–Chacay Melehue we recorded the best palaeomagnetic behaviours, in particular in the last locality where lithologies are of volcanic/volcaniclastic origin (Fig. 9). Component A bears a mean *in situ* direction at (Fig. 10) Dec=353, Inc=−74, $\alpha_{95}=4.5°$ whereas component B (Fig. 10) shows a mean *in situ* direction, in reverse polarity, at Dec=190, Inc=57, $\alpha_{95}=5.5°$, $k=14.0$, $N=52$ and a bedding-corrected mean at Dec=168.5, Inc=41, $\alpha_{95}=4.5°$, $k=19$, $N=52$ (Figs. 9 and 10), that is dissimilar to any other younger direction expected in the region.

In Rajapalo–Chacay Melehue, the basalts intercalated in the volcaniclastic sequence (Fig. 4, 60–75 m from the base) have X values which vary significantly (from $X=1\times10^{-4}$ to 1×10 SI) up-section, allowing the differentiation for the first time in the area, of at least five lava flows. On the basis of grain size, low-temperature oxidation and rapid cooling textures of titanomagnetites (Fig. 5c), we consider the mean direction of component B recorded in these basalts as the reference direction for the Pliensbachian magnetic field.

4.2.1. Field tests of palaeomagnetic stability

Component B in Puesto Araya and Rajapalo passes (Fig. 10) McFadden's [42] fold test (minimum test value at 100% of unfolding). Likewise, in Rajapalo it passes the reversal test [43] as a C class, whereas in Puesto Araya such test is "indeterminate" probably due to the scarcity of data in the reverse-polarity population. However, no significant deviations are observed in this locality between the normal and reverse populations. In addition in Rajapalo, the randomness directions test [44] applied in clasts from a conglomerate placed 80–90 m above the base (Fig. 4), indicates a positive (number of clasts=32, critical test value=11, test value=5.9) conglomerate test (Fig. 11) that provides solid evidence on the primary origin of the magnetisations recorded in the underlying beds.

Based on the solid evidence provided by optical observations and palaeomagnetic field tests, we conclude component B in Puesto Araya and Rajapalo is the characteristic magnetisation, that it was acquired during or shortly after the deposition (extrusion) of the sediments (lavas) in the Pliensbachian–Toarcian.

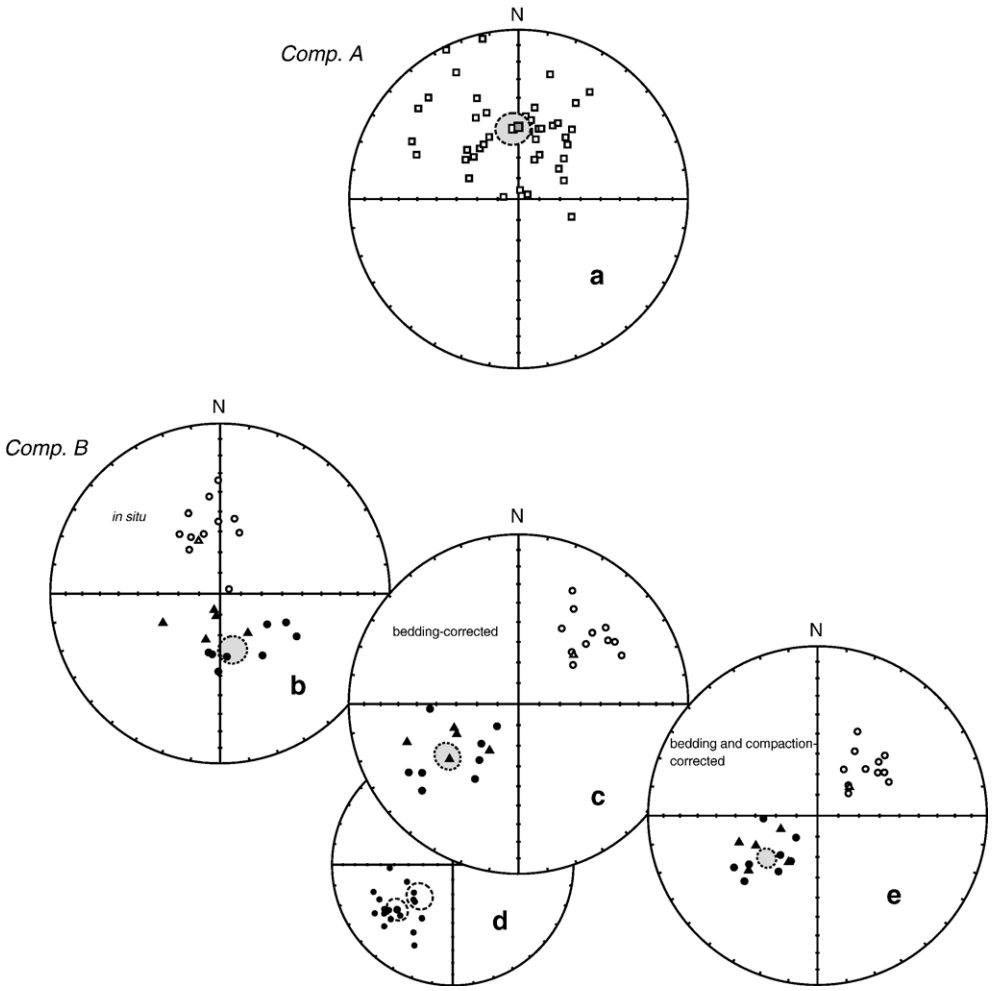

Fig. 7. Stereoplots showing magnetic directions from the Hettangian–Sinemurian localities. Component A yields a) *in situ* directions with normal polarity only which is very similar (Dec=355, Inc=−56, α_{95}=8°) to the present-day local field, whereas B is depicted b) *in situ* c) bedding-corrected and e) bedding- and inclination error-corrected, with opposite polarities and antiparallel directions. Note that bedding-corrected directions (here shown in reverse polarity) fall d) into two well-distinguishable groups, one with high inclinations recorded in the sills (diamonds) and the other with lower inclinations recorded in the sedimentary rocks (circles). Symbols: full (open) symbols = lower (upper) hemisphere; circles (triangles) = directions at Arroyo Malo (Las Chilcas); gray square = direction of present-day local magnetic field; gray circle = 95% confidence circle in reverse polarity (component B).

For component *A* the calculated PP is located at 61° E, 88.5° S, A_{95}=3.5°, N=262 whereas for component B, VGP (Table 2) yield a Pliensbachian–Toarcian palaeopole at 67° E, 74° S, A_{95}=5°, N=52 (Table 3).

5. Discussion

The construction of a Jurassic APW path for stable South America has always been a controversial subject since data are scarce and often, questionable. It is a fact that most Jurassic palaeopoles for the continent in the global palaeomagnetic database have been obtained using either old demagnetisation and analytical techniques, or bear no palaeomagnetic field tests. Yet, many of them are widely used to construct the continent's APW path. On the other hand, since they all fall close to the geographic pole, it is accepted that no polar wander has occurred in South America from the Middle to Late Mesozoic [e.g. 13–16]. New palaeomagnetic data derived from marine strata in southern South America indicate that this would not be entirely correct [11,12,17].

In order to construct the Jurassic APW path for South America (Fig. 12), we used the two new palaeopoles in our study and a few selected palaeomagnetic poles from the literature (Table 3). The latter were required to pass minimum reliability criteria, such

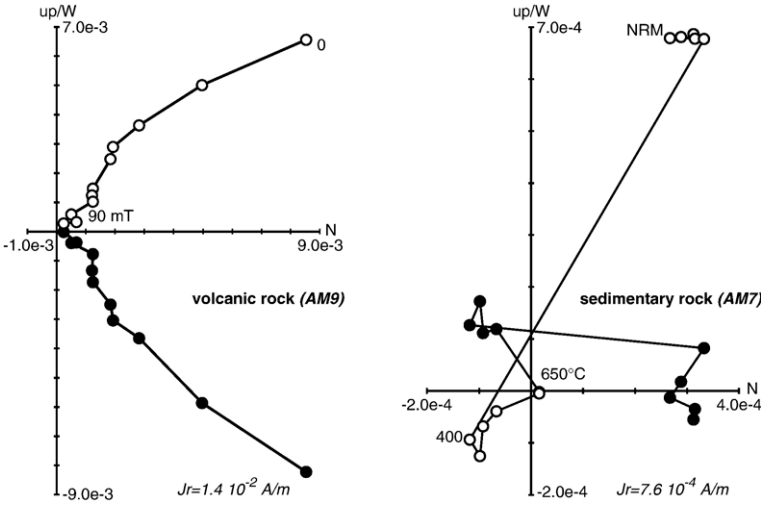

Fig. 8. At Arroyo Malo, component B passes a "baked contact test" at site 430 m (AM 10, Fig. 3). There, host sedimentary rocks (AM 7.3) carry two components, a soft with normal polarity acquired most likely during the intrusion of the sill (AM 9) and B, with reverse polarity. Symbols as in Fig. 6.

as: i) well dated sections, ii) unsuspected of undergoing vertical rotations, iii) full demagnetisation and vectorial analysis of the palaeomagnetic data, and iv) rock magnetic studies and/or palaeomagnetic field tests to constrain origin of magnetisation. As a consequence, most of the Jurassic South American published poles were not considered in the APW path in our study (Table 4). Among the most widely used in the literature, we excluded the Early Jurassic poles from the Bolivar Dykes in Venezuela and those of French Guyana that bear no field tests and which, despite their close age show different geographical positions yet not well understood. For the Middle Jurassic, we ruled out poles obtained in the volcanic Maranhao Formation from Brazil and in the Marifil volcanic Complex from SE Argentina (also recalculated in [12]) which bear no field tests, the pole obtained in the Mamil Choique Dykes from SE Argentina dated as Middle Jurassic that according to the authors, can be slighty rotated clockwise by the Gastre Fault and finally, the pole derived from the Middle Jurassic Chon Aike Complex in SE Argentina (also recomputed in [15,12]) which bears no field tests and no polarity reversals coinciding with a time of constant polarity changes of the Earth's magnetic field.

The palaeopoles in our APW path on the other hand, comprise the Late Triassic pole *1* obtained in the Los Colorados sedimentary/volcanic sequence from W Argentina that passes several palaeomagnetic field tests. For the Early Jurassic, we include pole *2* obtained in the volcanic Anari–Tapirapuã Formations from Brazil bearing rock magnetic studies, the Hettangian–Sinemurian pole in our study *3*, pole *4* derived from the Pliensbachian Lepá–Osta Arena volcanic/sedimentary Formation from SW Argentina with a positive fold test and finally, the Pliensbachian–Toarcian pole in our study *5*. Pole *3c* in Fig. 12 shows the Hettangian–Sinemurian pole in our study with bedding-correction only (no compaction-correction) falling further away from the Hettangian–Sinemurian poles. For the Middle

Table 3
Selected palaeomagnetic poles of stable South America (Fig. 12)

Rock unit/locality	Lithology	Age (Ma)/stage	Lat. S	Long. E	A_{95} dp/dm	Reference
1-Los Colorados Fm.	Volcanics/sediments	Late Triassic	76.0	280.0	8°	[45]
2-Anari-Tapirapua Fm.	Volcanics	196.6±0.4	65.5	250.0	3.5°	[46]
3-Comp. B-Mendoza	Sediments/volcanics	Hettangian–Sinemurian	51.0	223.0	6°	This study
4-Lepá-Osta Arena Fm.	Sediments/volcanics	Pliensbachian	75.5	129.5	6°	[12]
5-Comp. B-Mendoza-Neuquen	Sediments/volcanics	Pliensbachian–Toarcian	74.0	67.0	5°	This study
6-Marifil Complex	Volcanics	168–178	83.0	138.0	9°	[10]
7-El Quemado Complex (N of 48 °S)	Volcanics	153–157	81.0	172.0	5.5°	[10]

A_{95} = confidence limits of paleopoles.

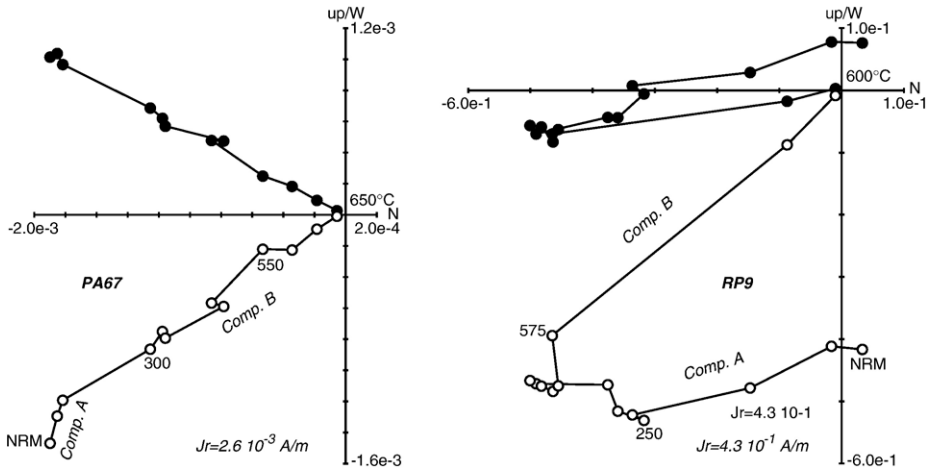

Fig. 9. Representative Zijderveld plots (bedding-corrected) from Pliensbachian–Toarcian sedimentary (PA67.3) and volcanic (RP9.1) rocks carrying components A and B. The latter shows N (S) declinations with negative (positive) inclinations and is carried by single to pseudo-single size titanomagnetites. Symbols as in Fig. 6.

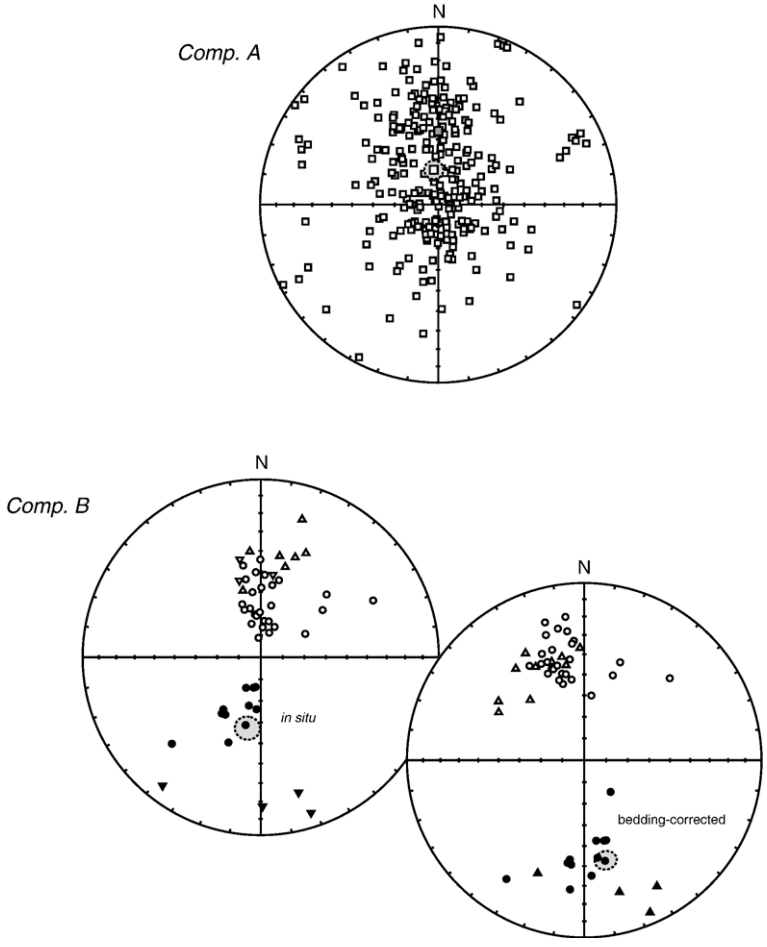

Fig. 10. Stereoplots from the Pliensbachian–Toarcian localities. Component A shows *in situ* sample directions with normal polarity only which is very similar (Dec=353, Inc=−74, α_{95}=4.5°) to the expected present-day local field, whereas those of B yields b) *in situ* and c) bedding-corrected, with opposite polarities and antiparallel directions. Symbols: as in Fig. 7; circles (triangles) = mean site directions at Rajapalo–Chacay Melehue (Puesto Araya).

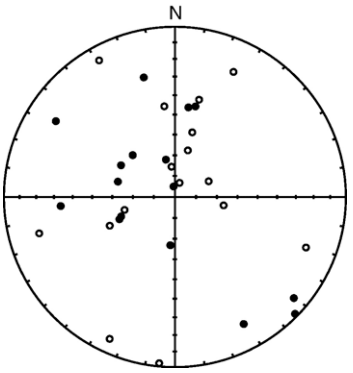

Fig. 11. The Pliensbachian succession at Rajapalo bears a positive conglomerate test (site 80 to 90 m, Fig. 4) that provides a solid support to the primary origin of the isolated magnetisations. Symbols as in Fig. 7.

Jurassic, we consider pole *6* obtained in the Marifil volcanic Complex from SE Argentina that passes the reversal test and finally for the Late Jurassic, pole *7* obtained in the El Quemado volcanic Complex which passes several field tests.

Results show there has been significant apparent polar wander for South America from the Late Triassic to the Middle Jurassic. The new Early Jurassic poles moreover, derive from sampling sites separated by 10 km (localities AM and LC for *3*) to 250 km (PA and RP for *5*), which would strongly support that the distance between the poles is not due to local tectonics.

Because South America was part of Pangea at that time, we considered finding the Early Jurassic cusp in other blocks of the supercontinent. Thus, we constructed the Mesozoic APW path for Eurasia (Fig. 13) using the data published in Torsvik et al. [52], and reassigned pole ages according to [47]. The path was translated to South American geographical coordinates using two classical palaeoreconstructions for Pangea: 1) Srivastava and Tapscott [53] to move Eurasia to North America, Klitgord and Schouten [54] to move North America to South Africa and Rabinowitz and La Breque [55] to move South Africa to South America, and 2) the model from Lawver and Scotese [56] that rotates Eurasia to North America, North America to Africa and Africa to South America. In general terms, the first model regards Africa as two different plates by the Jurassic whereas the second model interprets the continent as a single plate. Each palaeoreconstruction was tested on both groups of poles, i.e. Triassic to Sinemurian and Pliensbachian to Late Jurassic. The best statistical fit in the older group was achieved when applying the first model whereas the second model was the best in the case of the younger group, suggesting that Africa was already a single plate by the Middle Jurassic. In any case, both the Eurasian and the South America paths show a cusp recording the northward motion of the continents throughout the Early Jurassic, and subsequent displacement toward the south. The cessation of the northward motion of Pangea observed at the end of the Early Jurassic followed by counterclockwise rotation, could have been the result of the collision of the supercontinent with another terrain along its northern border [57].

Using the palaeopoles of our APW path (Table 3), palaeolatitudes (Fig. 14) and minimum drift rates of the Neuquén Basin (37.3° S, 70.5° W) were calculated. These indicate that, during the Late Triassic and lowermost Jurassic, the area was located further to the south than it is nowadays, i.e. at 50° S, and was moving northward at about 20 cm yr^{-1} until it reached its northernmost position, i.e. 25° S by the Late Early Jurassic. Subsequently, the basin moved southward again at 10 cm yr^{-1} and located at *c.* 30° S, where it stayed until the end of the Jurassic.

Drift rates between the Sinemurian and Pliensbachian (*c.* 20 cm yr^{-1}) may appear high but are quite comparable to those estimated for the break-up of Rodinia in the Neoproterozoic. Driving mechanisms that could prompt a supercontinent to move at a high rate are still controversial, although authors seem to

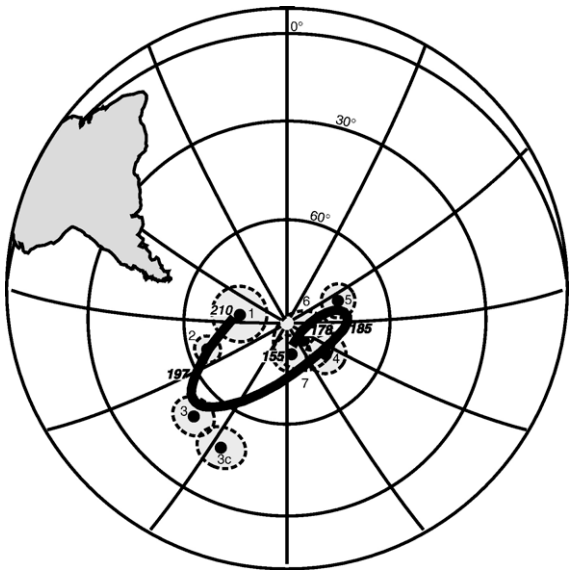

Fig. 12. Proposed APW path of stable South America for the Late Triassic–Late Jurassic, suggesting significant apparent polar wander between the Late Triassic and Middle Jurassic. 1–7: palaeomagnetic poles from Table 3; 3c: pole 3 without the inclination error-correction, falling away from the other Hettangian–Sinemurian poles; *210–155*: ages according to [47].

Table 4
Other poles of South America that are mentioned in the text

Rock unit/locality	Lithology	Age (Ma)/Stage	Lat. S	Long. E	A_{95} dp/dm	Reference
Bolivar Dykes	Volcanics	200–205	66.9	65.6	4.9°	[48]
French Guyana 2	Volcanics	198.3±2	73.2	195.3	3.4°	[49]
French Guyana 1	Volcanics	192.3±1.5	81.6	269.1	4.2°	[49]
West Maranhao	Volcanics	173–177	85.3	82.5	9.3°	[50]
Marifil complex	Volcanics	168–188	77.7	133.4	19°	[51]
Mamil choique dykes	Volcanics	~170	70.2	190.4	9.7°	[9]
Chon aike complex	Volcanics	165–175	85.0	17.0	4.9°	[8]

accept two major models. One explains the supercontinent's high rate on the basis of true polar wander [58,59], while the other model focuses on the occurrence of thermal instabilities beneath the lithosphere originated by deep-seated mantle plumes [60–62].

Finally, the latitudinal movements observed in South America and Eurasia during the Late Triassic–Middle Jurassic are highly consistent with paleobiogeographical data from both regions, usually attributed to other factors [63–65]. Thus, during the Hettangian–Sinemurian in the Southern Andes the South Pacific bivalve fauna attained its northernmost latitude, while by the Pliensbachian–Toarcian it had shifted southwards [63,64]. In addition in the Neuquén Basin the Pliensbachian marked the first expansion of colonial corals. Meanwhile, in the Northern Hemisphere, ammonites of the Boreal Realm, which dwelled at high latitudes spread southwards during the Pliensbachian [66]. Provincialism of the boreal ammonite fauna decreased between the Toarcian and Bajocian, to increase again by the Late Bajocian–Callovian, when the boreal fauna began to spread southwards [67,65].

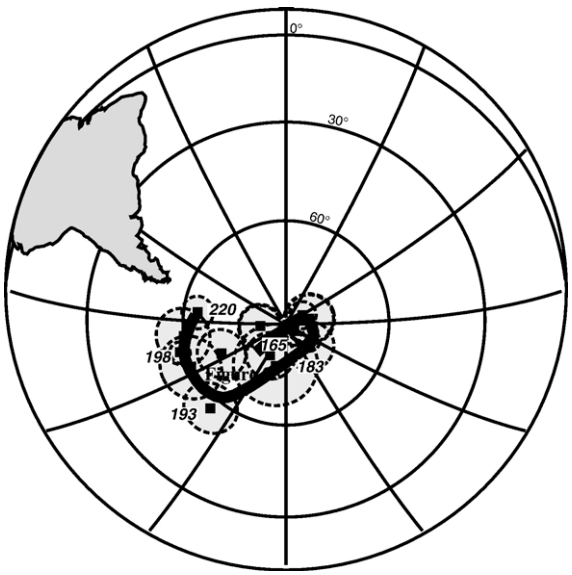

Fig. 13. The APW path of Eurasia for the Late Triassic–Late Jurassic, using the data from Torsvik et al. [52] and ages according to [47], shows strong similarities to the path in Fig. 12. Rotation of Eurasian poles to South American geographical coordinates was achieved using model 1) for the Triassic–Sinemurian (220–193 Ma) and model 2) for the Pliensbachian–Late Jurassic (183–165 Ma).*Model 1*: EU–NA by Srivastava and Tapscott [53], NA–SAF by Klitgord and Schouten [54] and SAF–SAM by Rabinowitz and La Breque [55] Model 2: EU–NA, NA–AF, AF–SAM by Lawver and Scotese [56].

6. Conclusions

Four ammonite-bearing sections from the Neuquén Basin, west-central Argentina, comprising sedimentary and volcanic rocks were sampled for palaeomagnetic studies. Ammonite Zones from the Andes were correlated with the Tethys Standard Zone, thus establishing a precise dating of sampling sites. Two magnetic components were identified, one soft (A) that represents most likely a present-day remagnetisation and another (component B), carried mainly by titanomagnetite and subordinately by titanohaematite, that is interpreted as the original Jurassic magnetisation, based on optical observations and palaeomagnetic field tests. Component B yielded two Early Jurassic PP, one for the Hettangian–Sinemurian located at 223° E, 51° S, A_{95}=6°, N=25 and another for the Pliensbachian–Toarcian, at 67° E, 74° S, A_{95}=5°, N=52. These palaeopoles were combined with others from the literature to construct a refined Mesozoic APW path from stable South America. Results show the continent underwent significant apparent polar wander between the Late Triassic and Middle Jurassic, in opposition with the stationary model widely accepted for that time interval. Calculated palaeolatitudes and minimum drift rates of the Neuquén Basin indicate that during the Late Triassic–lowermost Jurassic it was positioned at its southernmost latitudes. After the Sinemurian, the region moved northward at relatively high rates until by the end of the Early

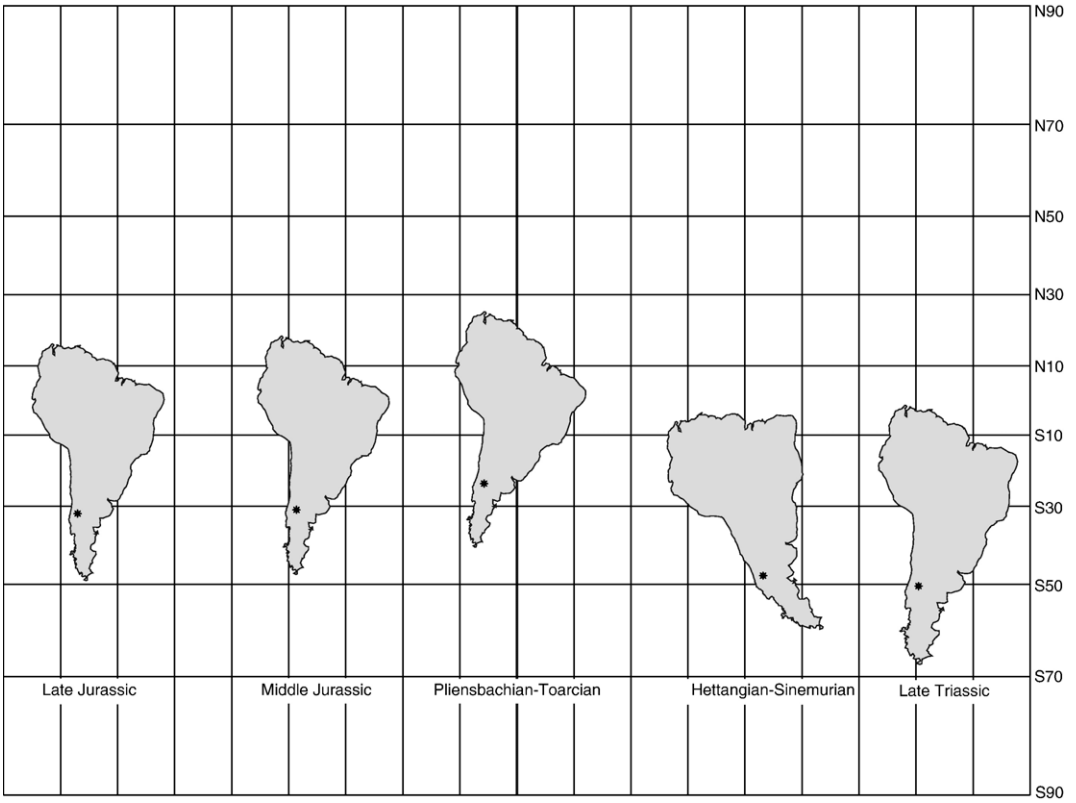

Fig. 14. Using the palaeopoles in Table 3, drift rates and paleolatitudes of the Neuquén Basin were calculated. Data show that by the end of the Triassic until the end of the Sinemurian the region was placed at its southernmost position (*c.* 50 °S). From then on, it moved northward at about 20 cm yr^{-1} and reached its furthermost location (*c.* 25° S) in the Pliensbachian. Subsequently, the area moved again to the south at 10 cm yr^{-1}. and eventually attained similar present-day positions (*c.* 30° S) by the end of the Jurassic.

Jurassic it reached its northernmost position. By the Toarcian, it began to move southward again until in the Middle Jurassic it situated close to present-day latitudes. These latitudinal movements are observed in other blocks from Pangaea, like Eurasia. Moreover, marine palaeobiogeographical data from South America and Eurasia are highly consistent with the latitudinal changes observed in different blocks from Pangaea.

Acknowledgements

The authors are indebted to the Argentinian Research Council (CONICET, PIP 2702,5635) and the INGEO-DAV (Buenos Aires University) The first author would like to acknowledge Dr. H. Vizán for his invaluable assistance during the field work and subsequent palaeomagnetic analysis, Dr. S. Damborenea and Dr. M. Manceñido for his contribution in the field, and Dr. R. Andreis for his contribution with the petrographical description. In addition, the authors would like to acknowledge Dr. A. Rapalini as well as Dr. K. Kodama and an anonymous reviewer for their comments and corrections which greatly helped to improve the quality of the original manuscript.

References

[1] S.R. May, R.F. Butler, North American Jurassic apparent polar wander: implications for plate motion, paleogeography and cordilleran tectonics, J. Geophys. Res. 91 (1986) 11519–11544.
[2] R. Van der Voo, Jurassic paleopole controversy: contributions from the Atlantic-bordering continents, Geology 20 (1992) 975–978.
[3] M.C. Van Fossen, D.V. Kent, High-Latitude Paleomagnetic Poles from Middle Jurassic Plutons and Moat Volcanics in New England and the Controversy Regarding Jurassic Apparent Polar Wander for North America, J. Geophys. Res. 95 (B11) (1990) 17503–17516.
[4] V. Courtillot, J. Besse, H. Théveniaut, North American Jurassic apparent polar wander: the answer from other continents? Phys. Earth Planet. Inter. 82 (1994) 87–104.
[5] S.E. Geuna, R. Somoza, H. Vizán, E.G. Figari, C.A. Rinaldi, Paleomagnetism of Jurassic and Cretaceous rocks in central Patagonia: a key to constrain the timing of rotations during the breakup of southwestern Gondwana? Earth Planet. Sci. Lett. 181 (2000) 145–160.

[6] D.A. Valencio, J.F. Vilas, Palaeomagnetism of some Middle Jurassic lavas from South-east Argentina, Nature 225 (5229) (1970) 262–264.
[7] K.M. Creer, J.G. Mitchell, J. Abou Deeb, Palaeomagnetism and radiometric age of the Jurassic Chon-Aike Formation from Santa Cruz province, Earth Planet. Sci. Lett. 14 (1972) 131–138.
[8] J.F. Vilas, Palaeomagnetism of some igneous rocks of the Middle Jurassic Chon-Aike Formation from Estancia La Reconquista, Province of Santa Cruz, Argentina, Geophys. J. R. Astron. Soc. 39 (1974) 511–522.
[9] A.E. Rapalini, M. López de Lucchi, Paleomagnetism and magnetic fabric of Middle Jurassic dykes from Western Patagonia, Argentina, Earth Planet. Sci. Lett. 120 (2000) 11–27.
[10] M.P. Iglesia Llanos, R. Lanza, A.C. Riccardi, S. Geuna, M.A. Laurenzi, R. Ruffini, Palaeomagnetic study of the El Quemado complex and Marifil formation, Patagonian Jurassic igneous province, Argentina, Geophys. J. Int. 154 (2004) 599–617.
[11] M.P. Iglesia Llanos, Magnetoestratigrafía y Paleomagnetismo del Jurásico Inferior marino de la Cuenca Neuquina, República Argentina, Ph.D. thesis, Universidad de Buenos Aires, Buenos Aires, 1997.
[12] H. Vizán, Paleomagnetism of the Lower Jurassic Lepá and Osta Arena Formations, Argentine, Patagonia, J. South Am. Earth Sci. 11 (1998) 333–350.
[13] D.A. Valencio, J.F. Vilas, I.G. Pacca, The significance of the palaeomagnetism of Jurassic–Cretaceous rocks from South America: predrift movements, hairpins and Magnetostratigraphy, Geophys. J. R. Astron. Soc. 73 (1983) 135–151.
[14] E. Oviedo, J.F. Vilas, Movimientos recurrentes en el Permo–Triásico entre el Gondwana Occidental y el Oriental, Actas 9° Congreso Geológico Argentino 3, Buenos Aires, 1984, pp. 97–114.
[15] A.E. Rapalini, A.L. Abdeldayem, D.H. Tarling, Intracontinental movements in Western Gondwanaland: a palaeomagnetic test, Tectonophysics 220 (1993) 127–139.
[16] M.E. Beck Jr., Jurassic and Cretaceous apparent polar wander relative to South America: Some tectonic implications, J. Geophys. Res. 104 (1999) 5063–5067.
[17] D.E. Randall, A new Jurassic–Recent apparent polar wander path for South America and a review of central Andean tectonic models, Tectonophysics 299 (1998) 49–74.
[18] M.A. Uliana, K.T. Biddle, Mesozoic–Cenozoic paleogeographical and geodynamic evolution of southern South America, Rev. Bras. Geocienc. 18 (1988) 172–190.
[19] R. Manceda, D. Figueroa, Inversion of the Mesozoic Neuquén Rift in the Malargüe Fold and Thrust Belt, Mendoza, Argentina, in: A.J. Tankard, R. Suárez Soruco, H.J. Welsink (Eds.), Petroleum Basins of South America, Am. Assoc. Petr. Geol., Memoir, vol. 62, The American Association of Petroleum Geologists, Tulsa, 1995, pp. 369–382.
[20] G.D. Vergani, A.J. Tankard, H.J. Belotti, H.J. Welsink, Tectonic evolution and paleogeography of the Neuquén Basin, Argentina, in: A.J. Tankard, R. Suárez Soruco, H.J. Welsink (Eds.), Petroleum Basins of South America, Am. Assoc. Petr. Geol., Memoir, vol. 62, The American Association of Petroleum Geologists, Tulsa, 1995, pp. 383–402.
[21] L. Legarreta, C.A. Gulisano, Análisis estratigráfico de la Cuenca Neuquina (Triásico superior–Terciario inferior), in: G.A. Chebli, L.A. Spalletti (Eds.), Cuencas Sedimentarias Argentinas, Serie de Correlación Geológica, vol. 6, Instituto Miguel Lillo, Universidad Nacional de Tucumán, San Miguel de Tucumán, 1989, pp. 221–244.
[22] M.P. Iglesia Llanos, A.C. Riccardi, The Neuquén composite section: magnetostratigraphy and biostratigraphy of the marine lower Jurassic from the Neuquén basin (Argentina), Earth Planet. Sci. Lett. 181 (2000) 443–457.
[23] S. Lanés, Late Triassic to Early Jurassic sedimentation in northern Neuquén Basin, Argentina: Tectosedimentary Evolution of the First Transgression, Acta Geol. 3 (2005) 81–106.
[24] A.C. Riccardi, S.E. Damborenea, M.O. Manceñido, S.C. Ballent, Hettangiano y Sinemuriano marinos en la Argentina, Actas 4° Congreso Geológico Chileno, Santiago de Chile, 1988, pp. C359–C374.
[25] A.C. Riccardi, S.E. Damborenea, M.O. Manceñido, S.C. Ballent, Hettangian and Sinemurian (Lower Jurassic) biostratigraphy of Argentina, J. South Am. Earth Sci. 4 (1991) 159–170.
[26] A.C. Riccardi, M.P. Iglesia Llanos, Primer hallazgo de un amonite triásico en Argentina, Rev. Asoc. Geol. Argent. 54 (1999) 298–300.
[27] A.C. Riccardi, S.E. Damborenea, M.O. Manceñido, M.P. Iglesia Llanos, The Triassic/Jurassic Boundary in the Andes of Argentina, Riv. Ital. Paleontol. Stratigr. 110 (2003) 69–76.
[28] P.N. Stipanicic, M.I.R. Bonetti, Posiciones estratigráficas y edades de las principales floras jurásicas argentinas, Ameghiniana 7 (1970) 57–78.
[29] W. Volkheimer, Descripción Geológica de la Hoja 27b, Cerro Sosneado, Provincia de Mendoza, vol. 151, Servicio Geológico Nacional, Buenos Aires, 1978, pp. 1–85.
[30] A.C. Riccardi, The Jurassic of Argentina and Chile, in: M. Moullade, A.E.M. Naim (Eds.), The Phanerozoic Geology of the world II, The Mesozoic B, Elsevier, Amsterdam, 1983, pp. 201–203.
[31] A.v. Hillebrandt, Liassic ammonite zones of South America and correlation with other provinces. With description of new genera and species of ammonites, in: W. Volkheimer (Ed.), Bioestratigrafía de los Sistemas regionales del Jurásico y Cretácico de América del Sur, Mendoza, 1987, pp. 111–157.
[32] G.E.G. Westermann, A.C. Riccardi, Middle Jurassic ammonite evolution in the Andean province and emigration to Tethys, in: U. Bayer, A. Seilacher (Eds.), Sedimentary and Evolutionary Cycles, Springer Verlag Lecture Notes on Earth Sciences, vol. 1, Springer-Verlag, Berlin, Heidelberg, New York, Tokyo, 1985, pp. 6–34.
[33] L. Clavijo, Estudio estratigráfico y tectónico del extremo austral de la Cordillera del Viento, Territorio del Neuquén, Ph.D. thesis, Facultad de Ciencias Naturales y Museo, Universidad Nacional de La Plata 60, La Plata, 1944.
[34] S.E. Damborenea, Early Jurassic Bivalvia of Argentina Pt.1, Stratigraphical Introduction and Superfamilies Nuculanacae, Arcaceae, Mytilaceae and Pinnacea, Palaeontographica A 199 (1987) 23–111 (Stuttgart).
[35] C.A. Gulisano, A. Gutiérrez Pleimling, The Jurassic of the Neuquén Basin. b) Mendoza Province, Asoc. Geol. Argent. Ser. E3 (1995) 1–103.
[36] J.L. Kirschvink, The least-squares line and plane and the analysis of palaeomagnetic data, Geophys. J. R. Astron. Soc. 62 (1980) 699–718.
[37] R.A. Fisher, Dispersion on a sphere, Proc. R. Soc. Lond. Ser. A 217 (1953) 295–306.
[38] G.L. Anson, K.P. Kodama, Compaction-induced inclination shallowing of the post-depositional remanent magnetization in a synthetic sediment, Geophys. J. R. Astron. Soc. 88 (1987) 673–692.
[39] J.P. Hodych, S. Bijaksana, R. Pätzold, Using magnetic anisotropy to correct for paleomagnetic inclination shallowing in some

magnetite-bearing deep-sea turbidites and limestones, Tectonophysics 307 (1999) 191–205.
[40] X. Tan, K. Kodama, An analytical solution for correcting palaeomagnetic inclination error, Geophys. J. Int. 152 (2003) 228–236.
[41] R.F. King, Remanent magnetism of artificially deposited sediments, Mon. Not. R. Astron. Soc. Geophys. Suppl. (7) (1955) 115–134.
[42] P.L. McFadden, A new fold test for palaeomagnetic studies, Geophys. J. Int. 103 (1990) 163–169.
[43] P.L. McFadden, M.W. McElhinny, Classification of the reversal test in palaeomagnetism, Geophys. J. Int. 103 (1990) 725–729.
[44] G. Watson, A test for randomness of directions, Mon. Not. R. Astron. Soc. Geophys. Suppl. (7) (1956) 160–161.
[45] H. Vizán, R. Ixer, P. Turner, J.M. Cortés, G. Cladera, Paleomagnetism of Upper Triassic rocks in the Los Colorados hill section, Mendoza province, Argentina, J. South Am. Earth Sci. 18 (2004) 41–59.
[46] C.R. Montes Lauar, I.G. Pacca, A.J. Melfi, E.M. Piccirillo, G. Bellieni, R. Petrini, R. Rizziri, The Anari and Tapirapuâ Jurassic formations, western Brazil: paleomagnetism, geochemistry and geochronology, Earth Planet. Sci. Lett. 128 (1994) 357–371.
[47] J. Ogg, The Jurassic Period, in: F. Gradstein, J. Ogg, A. Smith (Eds.), A Geologic Time Scale, Cambridge University Press, Cambridge, 2004, pp. 307–343.
[48] W.D. MacDonald, N.D. Opdyke, Triassic palaeomagnetism of northern South America, Am. Assoc. Pet. Geol. Bull. 58 (1974) 208–215.
[49] S. Nomade, H. Théveniaut, Y. Chen, A. Pouclet, C. Rigollet, Paleomagnetic study of French Guyana Early Jurassic dolerites: hypothesis of a multistage magmatic event, Earth Planet. Sci. Lett. 184 (2000) 155–168.
[50] A. Schult, S.D.C. Guerreiro, Paleomagnetism of Mesozoic igneous rocks from the Maranhâo Basin, Brazil, and the time of opening of the South Atlantic, Earth Planet. Sci. Lett. 42 (1979) 427–436.
[51] M. Mena, Correlación Paleomagnética de diversos afloramientos del Complejo Marifil (provincia de Río Negro), Rev. Asoc. Geol. Argent. 45 (1990) 136–144.
[52] T.H. Torsvik, R. Van der Voo, J.G. Meert, J. Mosar, H.J. Walderhaug, Reconstructions of the continents around the North Atlantic at about the 60th parallel, Earth Planet. Sci. Lett. 187 (2001) 55–69.
[53] S.P. Srivastava, C.R. Tapscott, Plate kinematics of the North Atlantic, in: P.R. Vogt, B.E. Tucholke (Eds.), The Geology of North America, The Western North Atlantic Region, vol. M, Geol. Soc. Am., New York, 1986, pp. 379–404.
[54] K.D. Klitgord, H. Schouten, Plate kinematics of the central Atlantic, in: P.R. Vogt, B.E. Tulchoke (Eds.), The Geology of North America, The Western North Atlantic Region, vol. M, Geol. Soc. Am., New York, 1986, pp. 351–378.
[55] P.D. Rabinowitz, J. La Brecque, The Mesozoic South Atlantic Ocean and Evolution of its Continental Margins, J. Geophys. Res. 84 (1979) 5973–6002.
[56] L.A. Lawver, C.R. Scotese, A revised reconstruction of Gondwana, in: G.D. McKenzie (Ed.), Gondwana Six: Structure, Tectonics and Geophysics, Am. Geophys. Union, Geophys. Monogr., vol. 40, 1987, pp. 17–23.
[57] J.B. Edel, P. Duringer, The apparent polar wander path of the European plate in Upper Triassic–Lower Jurassic times and the Liassic intraplate fracturing of Pangea: new palaeomagnetic constraints from NW France and SW Germany, Geophys. J. Int. 128 (1997) 331–344.
[58] J.L. Kirschvink, R.L. Ripperdan, D.A. Evans, Evidence for a large-scale reorganization of Early Cambrian continental landmasses by interial interchange true polar wander, Science 277 (1997) 541–545.
[59] D.A. Evans, True polar wander, a supercontinental legacy, Earth Planet. Sci. Lett. 157 (1998) 1–8.
[60] M. Gurnis, Large-scale mantle convection and the aggregation and dispersal of supercontinents, Nature 332 (1988) 695–699.
[61] M. Gurnis, T.H. Torsvik, Rapid drift of large continents during the late Precambrian and Palaeozoic: palaeomagnetic constraints and dynamic models, Geology 22 (1994) 1023–1026.
[62] J.G. Meert, E. Tamrat, A mechanism for Explaining Rapid Continental Motion in the Late Neoproterozoic, in: P.G. Eriksson, W. Altermann, D.R. Nelson, W.U. Mueller, O. Catuneanu (Eds.), The Precambrian Earth: Tempos and Events, Developments in Precambrian Geology, vol. 12, Elsevier, Amsterdam, 2004, pp. 255–267.
[63] S.E. Damborenea, Palaeobiogeography of Early Jurassic Bivalves along the Southeastern Pacific Margin, Actas 13° Congreso Geológico Argentino y 3° Congreso de Exploración de Hidrocarburos, vol. 5, Asociación Geológica Argentina, Instituto Argentino del Petróleo y del Gas, Buenos Aires, 1996, pp. 151–167.
[64] S.E. Damborenea, Jurassic evolution of Southern Hemisphere marine palaeobiogeographic units based on benthonic bivalves, Geobios 35 (M.S. 24) (2002) 51–71.
[65] K.N. Page, Mesozoic Ammonoids in Space and Time, in: N.H. Landman, K. Tanabe, R.A. Davis (Eds.), Ammonoid Paleobiology, Planum Press, New York, 1996, pp. 755–794.
[66] F. Macchioni, F. Cecca, Biodiversity and biogeography of middle-late liassic ammonoids: implications for the Early Toarcian mass extinction, Geobios 35 (M.S. 24) (2002) 165–175.
[67] A.v. Hillebrandt, P. Smith, G.E.G. Westermann, J.H. Callomon, Ammonite zones of the circum-Pacific region, in: G.E.G. Westermann (Ed.), The Jurassic of the Circum-Pacific, Cambridge University Press, New York, 1992, pp. 247–272.